

# NUMERICAL MODELING OF COUPLED MOISTURE, SOLUTE AND HEAT TRANSPORT IN FROZEN SOILS

A.E. Sheshukov, A.G. Egorov

*Chebotarev Research Institute of Mathematics and Mechanics,  
Kazan State University,  
Universitetskaya 17, Kazan 420008, Russia  
e-mail: alexey.sheshukov@ksu.ru*

## Abstract

Frozen barriers in a porous medium represent zones with an increased ice content in pore voids. Creation of such barriers can be used as an effective tool for limiting moisture and contaminant transport in soils. We study in a local equilibrium formulation a one-dimensional problem that describes the dynamics of phase transitions at the interface between two water saturated porous domains with different temperatures and concentrations of solutes. To solve the resulting system of the equations we use a numerical fixed domain method based on a method of overrelaxation. The numerical experiments show the existence of three regimes. The first regime offers no frozen barrier formation, while in the other two regimes, a frozen barrier can be generated. Two types of frozen barriers are distinguished: static and dynamic. The first one is an ice-bonded zone which completely eliminates forced seepage. The second type represents a narrow frozen zone expanding with a rate proportional to  $x/\sqrt{t}$ , and allowing a small seepage flux through itself that is damped out in time as  $1/\sqrt{t}$ .

## Introduction

Permafrost is a soil system that remains below the freezing point of water continuously for two or more years. Migration of unfrozen pore water plays a major role in various natural and artificial phenomena in permafrost. Moisture flow induces heaving of soils, creates zones with an increased ice content, causes salt redistribution in frozen saline soils, etc. An extensive review of studies on soil freezing and migration processes associated with it was provided by O'Neill (1983).

The environmental impact of salt dissolved in pore water is very significant. Laboratory experiments (Chamberlain, 1983) have shown that frost heave in saline soils is reduced compared to the same soils containing relatively pure soil solution. Baker and Osterkamp (1989) studied experimentally the salt redistribution in a soil column during downward freezing. Their experiments revealed the existence of an ice-bonded interface between the frozen and unfrozen regions.

A mathematical model of coupled heat, moisture and solute transport in frozen soils was proposed by Entov et al. (1986) and Panday and Corapcioglu (1991). This model allows the presence of regions with ice-water coexistence that will be called two-phase zones. In such zones, the pore-water freezing temperature can be determined from a generalized Clapeyron-Clausius

equation (Prigogine and Defay, 1954). When salt molecules are present in a water solution, the freezing temperature is influenced by osmotic pressure effects (Loch, 1978). The thermodynamic equilibrium condition provides a linear relation between freezing temperature and concentration of solutes.

Panday and Corapcioglu (1991) used this model to describe solute rejection in freezing soils. Several problems for the freezing of saturated saline soils with insignificant influence of heat and solute convective fluxes were solved by Entov et al. (1986). The opposite situation when convection dominates over conduction and diffusion, was studied by Egorov et al. (1995). They considered an intensive pumping of water solution into an initially frozen porous medium.

In this paper, the model is used to simulate the transformation of an interface between unfrozen and frozen porous domains. The dynamics of phase transitions and solute redistribution causes not only thawing of ice in an initially "cooled" domain, but also the formation of a narrow zone with increased ice content near the interface. This zone represents an ice-formed barrier that prevents forced filtration in porous media. Such frozen barriers may be used in practice, for example, to immobilize contaminants within a porous medium, to prevent water and soil encroachment while a building foundation is put in place, etc.

A special technique for frozen barrier formation in permafrost was proposed by Mironenko et al. (1989). It consists of a consecutive injection of saline and fresh water. The concentrated salt solution is pumped into soil and causes some of interstitial ice to melt, and the associated latent heat reduces the temperature of the medium. When the following fresh water reaches the cooled medium, it can freeze and form a frozen barrier there. This paper concerns the existence criteria for such barriers.

## Mathematical model

A one-dimensional mathematical model is presented to simulate the processes occurring during freezing of the interface between two porous domains. It is assumed that the porous medium is non-deformable and that the ice is incompressible. Pore voids are assumed to be fully filled with ice and water solution, i.e., there is no air present.

At the initial time, let porous domain  $[-l, l]$  be divided by a plane  $x = 0$ . At  $x < 0$  there is unfrozen soil saturated by fresh water at a temperature higher than the freezing point of pure water. At  $x > 0$  there is a thermodynamically equilibrium frozen soil. One part of the pore void is filled with ice and the other part is filled with concentrated water solution.

The conservation of mass for unfrozen water and ice is given by

$$n \frac{\partial}{\partial t} (\rho_w S + \rho_i (1 - S)) + \rho_w \frac{\partial V}{\partial x} = 0 \quad [1]$$

where  $n$  is the porosity,  $S$  is the unfrozen water saturation,  $\rho$  is the density,  $V$  is the seepage velocity, and subscripts  $w, i$  indicate water and ice respectively.

The conservation of mass for salt dissolved in pore water is expressed by

$$n \frac{\partial Sc}{\partial t} + \frac{\partial cV}{\partial x} = nD \frac{\partial}{\partial x} S \frac{\partial c}{\partial x} \quad [2]$$

where  $c$  is the concentration of solute and  $D$  is the diffusion coefficient. Equation (2) assumes that ice crystals cannot incorporate molecules of salt (all solute is injected into the liquid phase).

The conservation of energy for the soil system can be expressed as

$$\frac{\partial}{\partial t} (C_m (T - T_f)) + \rho_i n L \frac{\partial S}{\partial t} + C_w \frac{\partial}{\partial x} (V (T - T_f)) = \frac{\partial}{\partial x} \lambda_m \frac{\partial T}{\partial x} \quad [3]$$

where  $T$  is the temperature,  $T_f = 0^\circ\text{C}$ , and  $L$  is the latent heat of fusion (assumed constant). The heat capacity  $C_m$  and the thermal conductivity  $\lambda_m$  of the system depend upon water saturation. The second term in (3) represents the heat released due to freezing of water.

In this study, it is assumed that the water solution and ice are in a state of equilibrium within a two-phase zone. For the sake of simplicity, we assume a linear dependence of temperature on concentration. In the unfrozen zone, the temperature is higher than the freezing point of the solute. This can be summarized by determining the zone's type (fully frozen, unfrozen, and two-phase) as

$$S \in H(\gamma c + T - T_f) \quad [4]$$

where  $H$  is the Heaviside step-function and  $\gamma$  is the cryoscopic constant (Everett, 1963). Equation (4) implies that for  $S=1$  the temperature is above the freezing point of the solute (unfrozen zone); for  $S = 0$  the temperature is below the freezing point of the solute (fully frozen zone);  $S \in (0, 1)$  - equilibrium condition  $T = T_f - \gamma c$  occurs (two-phase or frozen zone).

The Darcy's law is applied for liquid flow

$$V = -K \frac{\partial H}{\partial x} \quad [5]$$

where  $H$  is the hydraulic head. The hydraulic conductivity  $K(S)$  is specified as (Panday and Corapcioglu, 1991).

$$K(S) = K_0 S^m, \quad m > 1 \quad [6]$$

In the unfrozen zone  $K$  is equal to the saturated hydraulic conductivity  $K_0$ .

Equations (1)-(5) constitute the complete system of equations with five unknowns  $S, c, T, V, H$  that are subject to appropriate initial and boundary conditions

$$t = 0, \quad -1 < x < 0: \quad S = 1, \quad c = 0, \quad T = T_- \quad (T_- > T_f)$$

$$t = 0, \quad 0 < x < 1: \quad S = S_+, \quad c = c_+, \quad T = T_+ = T_f - \gamma c_+ \quad (0 < S_+ < 1, x)$$

$$x = -1: \quad S = 1, \quad c = 0, \quad T = T_-, \quad H = H_-$$

$$x = 1: \quad S = S_+, \quad c = c_+, \quad T = T_+, \quad H = H_+ \quad (H_- > H_+)$$

$$[7] [8] [9] [10]$$

Next, the numerical solution will be developed under the complementary simplifying assumptions

$$\rho_w = \rho_i, \quad C_w = C_i, \quad \lambda_w = \lambda_i \quad [11]$$

i.e., thermodynamic parameters of both phases of water are equal. Hence, the heat capacity  $C_m$  and the thermal conductivity  $\lambda_m$  are constant and equal to their average values. The validity of these assumptions was discussed in Egorov et al. (1995). Substituting (11) into (1) shows that seepage velocity  $V$  is independent of space coordinates and can be defined by integration of (5).

We now introduce dimensionless variables

$$\bar{x} = \frac{x}{l}, \quad \bar{t} = \frac{C_m l^2}{\lambda_m}, \quad \bar{T} = \frac{T_f - T}{T_0}, \quad \bar{c} = \frac{\gamma c}{T_0}, \quad \bar{V} = \frac{C_m l V}{n \lambda_m}, \quad T_0 = \frac{n \rho_i L}{C_m}$$

Then (1)-(10) can be rewritten in terms of these dimensionless variables as

$$\frac{\partial S \bar{c}}{\partial \bar{t}} + \bar{V} \frac{\partial \bar{c}}{\partial \bar{x}} = \varepsilon \frac{\partial}{\partial \bar{x}} S \frac{\partial \bar{c}}{\partial \bar{x}} \quad [12]$$

$$\frac{\partial}{\partial \bar{t}} (\bar{T} - S) + \beta \bar{V} \frac{\partial \bar{T}}{\partial \bar{x}} = \frac{\partial^2 \bar{T}}{\partial \bar{x}^2} \quad [13]$$

$$S \in H(\bar{c} - \bar{T}) \quad [14]$$

$$\bar{V} = \alpha \left( \int_{-1}^1 S^{-m} d\bar{x} \right)^{-1} \quad [15]$$

$$x = -1: \quad \bar{T} = \bar{T}_-, \quad \bar{c} = 0, \quad S = 1$$

$$x = 1: \quad \bar{T} = \bar{c} = \bar{T}_+, \quad S = S_+$$

$$t = 0: \quad \bar{T} = \begin{cases} \bar{T}_-, & x < 0 \\ \bar{T}_+, & x > 0 \end{cases}, \quad \bar{c} = \begin{cases} 0, & x < 0 \\ \bar{T}_+, & x > 0 \end{cases}, \quad S = \begin{cases} 1, & x < 0 \\ S_+, & x > 0 \end{cases}$$

where  $\varepsilon = DC_m/\lambda_m$ ,  $\beta = nC_w/C_m$ ,  
and  $\alpha = C_m K_0 (H_- - H_+) / (n \lambda_m)$ .

## Numerical solution

A finite-difference scheme, implicit in time, is used for the numerical solution of equations (12) and (13). The magnitude  $\bar{V}$  for each time-step is calculated from (15) using the known grid function of saturation in the previous time layer. Then system (12)-(15) is rewritten as

$$\begin{aligned} \frac{\bar{S}_i \bar{c}_i - \bar{S}_{i-1} \bar{c}_{i-1}}{\tau} + \frac{\bar{V}}{h_i} (\bar{c}_i - \bar{c}_{i-1}) - \frac{\varepsilon}{h_i} \left( S_i \frac{\bar{c}_{i+1} - \bar{c}_i}{h_{i+1}} - S_{i-1} \frac{\bar{c}_i - \bar{c}_{i-1}}{h_i} \right) &= 0 \\ \frac{\bar{T}_i - S_i - \bar{T}_{i-1} + \bar{S}_{i-1}}{\tau} + \frac{\beta \bar{V}}{h_i} (\bar{T}_i - \bar{T}_{i-1}) - \frac{1}{h_i} \left( \frac{\bar{T}_{i+1} - \bar{T}_i}{h_{i+1}} - \frac{\bar{T}_i - \bar{T}_{i-1}}{h_i} \right) &= 0 \\ S_i \in H(\bar{c}_i - \bar{T}_i) \\ \bar{V} = \alpha (\bar{S}^{-m}, 1)^{-1} + \delta \end{aligned} \quad [16] [17] [18] [19]$$

where  $\bar{x}_i = \bar{x}_i - \bar{x}_{i-1}$ ,  $\bar{x}_i = 0.5 (\bar{x}_i + \bar{x}_{i+1})$  and  $\tau$  is the time-step. Subscript  $i$  indicates that the space location is at node  $\bar{x}_i$ , and functions in previous time layer are denoted by the tilde. The inner product of grid functions is bracketed in (19). For the solution  $\bar{c}$  being determined within fully frozen zone, the small dimensionless quantity  $\delta$  ( $10^{-70}$  in calculations) has to be introduced in (19).

The rapid change of saturation is presumed to take place in a small zone close to  $\bar{x} = 0$ . Therefore, we use an essentially non-uniform grid. The grid is compressed inside the narrow zone  $\sim 10^{-2}$  near  $\bar{x} = 0$  and extended outside this zone with the increase of  $|\bar{x}|$ . The grid-step  $h_i$  is changed from  $10^{-4}$  near  $\bar{x} = 0$  to  $10^{-2}$  at  $|\bar{x}| = 1$ .

An iterative successive solution scheme (Ortega and Rheinboldt, 1970), such as a method of overrelaxation, solves (16)-(18) for  $S, \bar{T}, \bar{c}$ . These values are simultaneously calculated at each iteration from the system of equations

$$a S \bar{c} + b \bar{c} - d S = f_c, \quad e \bar{T} - S f_T, \quad S \in H(\bar{c} - \bar{T})$$

with constants  $a, b, d, e, f_c > 0$  and  $f_T$  depending on known values of grid functions. The solution of this system can be obtained explicitly. An iterative procedure proceeds until convergence in (16) and (17) is achieved. The sufficient condition for the existence and uniqueness of the solution is that  $\bar{c}$  does not decrease with  $\bar{x}(\bar{c}_{i+1} - \bar{c}_i \geq 0)$ .

We use a variable time-step  $\tau$  that is increased from  $10^{-8}$  at the beginning to  $10^{-6}$  at the end of calculations. The numerical procedure stops at time  $\bar{t} \sim 10^{-4}$  when the zone with rapid change of  $S$  exceeds the area of the compressed grid.

## Results and discussion

We conduct the numerical simulation for various values of unknown functions on the external boundaries:

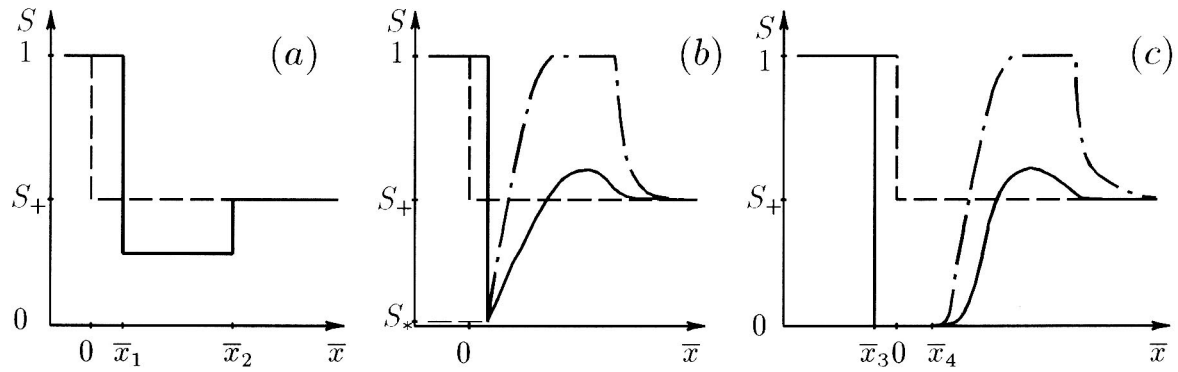


Figure 1. Saturation profile for different regimes. Initial saturation distribution is shown by dashed line.

value  $\bar{T}_-$  is kept constant, while  $S_+$  and  $\bar{T}_+$  are varied. The numerical experiments show the existence of three different regimes. Saturation profiles for these regimes are presented in Figure 1.

A solution for regime A comprises a superposition of two waves (points  $\bar{x}_1$  and  $\bar{x}_2$ ) which move to the right with a constant velocity (Figure 1a). Here convective fluxes dominate diffusion and conduction. This regime offers no ice-formed barrier formation. A complete analytical solution for this situation is given in Egorov et al. (1995).

Regime C offers a fully frozen zone  $[\bar{x}_3, \bar{x}_4]$  expanding in time as  $\sqrt{\bar{t}}$  (Figure 1c). For various  $S_+, \bar{T}_+$  at  $\bar{x} > \bar{x}_4$  we observe a two-phase zone as well as an unfrozen zone embedded in a two-phase one (chain line). The presence of the fully frozen zone eliminates forced convection as well as liquid flow in the system. Therefore, this regime can be called a "diffusive" one compared with "convective" regime A. The frozen barrier generated in this regime can be termed a static frozen barrier.

Regime B is an intermediate regime between regimes A and C. In it, there exists a narrow zone close to  $\bar{x} = 0$  with a small magnitude  $S_*$  of saturation (Figure 1b). The peak of the saturation profile within this zone occupies  $1 \div 2$  nodes, and the saturation profile is slightly expanded in time, replacing to the right. The numerical solution is similar to a self-similar solution with similarity variable  $\bar{x} / \sqrt{\bar{t}}$ , and the seepage flux decays as  $1 / \sqrt{\bar{t}}$  and is independent (!) of the external head gradient. Therefore, the main seepage resistance is concentrated in this zone, and a fine balance between convective and either conductive or diffusive fluxes is spontaneously maintained due to small variations of  $S_*$  around zero. The frozen barrier generated in this regime can be termed a dynamic frozen barrier.

Figure 2 is a regime map in plane  $(\bar{T}_+, S_+)$  for  $\bar{T}_- = 0.6$ . The map is subdivided into five domains.

Regimes A, B and C are realized within three corresponding domains independent of the choice of initial condition. The results of the numerical solution for two other domains depend on the initial saturation distribution. Regime A occurs within both domains if the initial saturation distribution does not contain values of the saturation function close to zero. In the opposite case, regimes B and C exist, respectively.

It can be seen that curves 1, 2 and 3 completely determine the regime map (Figure 2). Curve 1 is independent of  $\bar{T}_-$ . The corresponding dependence  $S_+ - (1 - \beta S_+) \bar{T}_+ = 0$  represents the criterion for non-existence of the "convective" solution, and it was obtained in Egorov et al. (1995).

The value  $\bar{T}_-$  significantly influences curves 2 and 3. These curves are plotted in Figure 3 for different and  $X \varepsilon = 0.003, \beta = 0$  and  $m = 2$ . Numbers 1 through 6 for curve 2 (Figure 3a) correspond to  $\bar{T}_- = 0; -0.2; -0.5; -1; -3; -\infty$ , respectively. When  $\bar{T}_- = -\infty$ , the curve 2 coincides with curve 1. Curve 2 is displaced to the right when  $\bar{T}_-$

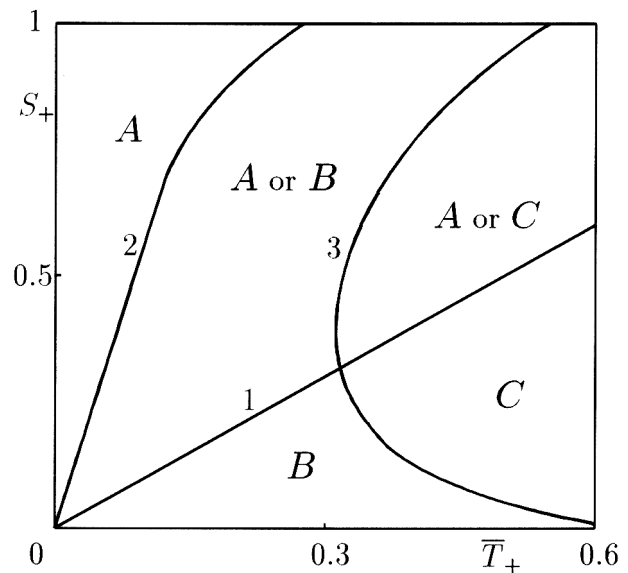


Figure 2. Regime map in plane  $(\bar{T}_+, S_+)$  subdivided into five domains.

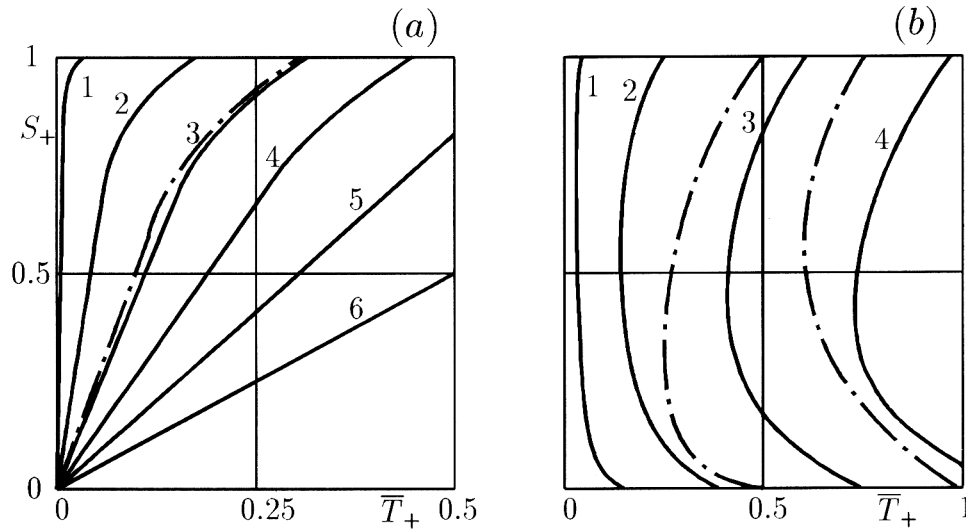


Figure 3. Curves 2 (a) and 3 (b) from Figure 2 for different  $\bar{T}_-$ .

increases and reaches its limit at  $\bar{T}_- = 0$ . We emphasize that frozen barrier can never be generated at  $\bar{T}_+$  close to zero for arbitrary  $\bar{T}_-$ . The numerical simulations show that curve 2 depends weakly on  $\epsilon$ . This dependence is shown in Figure 3a where a chain line is presented for  $\epsilon = 0$  and  $\bar{T}_- = -0.5$ .

Curve 3 is plotted in Figure 3b by solid lines for different  $\bar{T}_-$ . Numbers 1 through 4 correspond to  $\bar{T}_- = 0$ ;  $-0.2$ ;  $-0.5$ ;  $-0.8$ , respectively. The curve is displaced to the right up to infinity (for  $\bar{T}_- = -\infty$ ) when  $\bar{T}_-$  decreases. The parameter  $\epsilon$  significantly influences curve 3, in contrast to curve 2. Chain lines illustrate curve 3 computed for  $\bar{T}_- = -0.5$  and  $\epsilon = 0$  (left curve) and  $\epsilon = 0.01$ .

The numerical experiments show that the results obtained depend slightly on parameter  $\beta$  which is varied from 0 to 0.3.

The non-trivial numerical solution obtained makes the problem quite interesting from the theoretical point of view. An analytical method has to be derived for better understanding of the problem. Prior analytical results (Egorov and Sheshukov, 1997), based on the self-similar solutions, support the validity of the results presented in this paper.

## Summary and conclusions

A mathematical model is applied to simulate the transformation of the interface between two saturated porous domains with different temperatures and concentrations of solute. The model consists of mass balance equations for unfrozen water and solute, heat balance, thermodynamic equilibrium condition and Darcy's law. The numerical procedure is used to solve the resulting set of equations with some simplifying approximations. Numerical experiments show an existence of three different regimes. The first two regimes describe two limiting cases related to a large seepage flux (regime A) and a zero seepage flux (regime C). In the first case, diffusive and conductive fluxes dominate convective fluxes, while convective fluxes can be neglected in the second. The intermediate regime B offers a refinement balance of convective and conductive fluxes of heat and solute. The regime's map with five domains is plotted. Three observed regimes exist in three corresponding domains. In the other two domains the choice of which regime is realized depends on the initial saturation distribution. No barrier forms in regime A. Regimes B and C describe dynamic and static frozen barriers respectively. Existence criteria for each regime are obtained.

## References

- Baker, G.C. and Osterkamp, T.E. (1989). Salt redistribution during freezing of saline sand columns at constant rates. *Water Resources Research*, **25**, 1825-1831.
- Chamberlain, E.J. (1983). Frost heave of saline soils. In *Proceedings 4th International Conference on Permafrost, Fairbanks, Alaska*. National Academy Press, Washington, DC, pp. 121-126.
- Egorov A.G., Kosterin A.V. and Sheshukov A.E. (1995). One-dimensional problems of frozen soil thawing due to solution seepage. *Fluid Dynamics*, **30**, 767-775.
- Egorov A.G. and Sheshukov A.E. (1997). On frozen barrier within a saturated porous medium. *European Journal of Applied Mathematics*, (submitted).



- Entov, V.M., Macksimov, A.M. and Tsyppin, G.G.** (1986). Two-phase region formation during the crystallization of a mixture in porous media. *Dokl. Akad. Nauk SSSR*, **288**, 621-624.
- Everett, D.H.** (1963). *An Introduction to the Study of Chemical Thermodynamics*. Longmans Green and Co., London.
- Loch, J.P.G.** (1978). Thermodynamic equilibrium between ice and water in porous media. *Soil Science*, **126**, 77-80.
- Mironenko, V.M., Atroschenko, F.G. and Rumynin, V.G.** (1989). Method of ice-formed barrier generation. Patent No. 15079977. *Otkryt. Izobret.*, **34** (In Russian).
- O'Neill, K.** (1983). The physics of mathematical frost heave models: a review. *Cold Regions Science and Technology*, **6**, 275--291.
- Ortega, J.M. and Rheinboldt, W.C.** (1970). *Iterative solution of nonlinear equations in several variables*. Academic Press, New York.
- Panday, S. and Corapcioglu, M.Y.** (1991). Solute rejection in freezing soils. *Water Resources Research*, **27**, 99--108.
- Prigogine, I. and Defay, R.** (1954). *Chemical Thermodynamics*. Longmans Green and Co., London (543 pp).